Coherence and stiffness of spin waves in diluted ferromagnets

I. Turek[*]

Institute of Physics of Materials, Academy of Sciences of the Czech Republic, Žižkova 22, CZ-616 62 Brno, Czech Republic

J. Kudrnovský[†] and V. Drchal[‡]

Institute of Physics, Academy of Sciences of the Czech Republic, Na Slovance 2, CZ-182 21 Praha 8, Czech Republic

We present the results of a numerical analysis of magnon spectra in supercells simulating two-dimensional and bulk random diluted ferromagnets with long-range pair exchange interactions. We show that low-energy spectral regions for these strongly disordered systems contain a coherent component leading to interference phenomena manifested by a pronounced sensitivity of the lowest excitation energies to the adopted boundary conditions. The dependence of configuration averages of these excitation energies on the supercell size can be used for an efficient determination of the spin-wave stiffness D. The developed formalism is applied to the ferromagnetic Mn-doped GaAs semiconductor with optional incorporation of phosphorus; the obtained concentration trends of D are found to be in reasonable agreement with recent experiments. Moreover, a relation of the spin stiffness to the Curie temperature T_C has been studied for Mn-doped GaAs and GaN semiconductors. It is found that the ratio T_C/D exhibits qualitatively the same dependence on Mn concentration in both systems.

I. INTRODUCTION

Magnon spectra of ferromagnetic systems represent a subject of long-lasting theoretical and experimental research, motivated by the well-known relevance of magnons for finite-temperature properties and for the magnetization dynamics on a microscopic scale. Qualitative and quantitative features of the magnon spectra become especially important for recently investigated low-dimensional systems, such as ultrathin films and nanowires, as well as for disordered or diluted bulk systems, such as metallic solid solutions and diluted magnetic semiconductors.

On the theoretical side, the simplest approaches to the magnon spectra employ various Heisenberg Hamiltonians with pair exchange interactions between localized spins. The resulting equations of motion for spin excitations are solved by means of the Tyablikov decoupling procedure (random-phase approximation, RPA) [1,2], which yields an improved description compared to the usual mean-field approximation (MFA). For finite-temperature properties, other methods of statistical physics, including Monte Carlo simulations, can be used as well.

The treatment of magnons in random ferromagnets with crystalline structures is obviously more difficult than in the case of perfect nonrandom crystals since the spin waves propagate through a random system even at zero temperature. In analogy with realistic models of lattice vibrations (phonons), the disorder in the effective Hamiltonian for the magnon dynamics, i.e., the dependence of the Hamiltonian matrix elements on the occupation of lattice sites by various atomic species of the random alloy, is quite complicated as a consequence of the Goldstone sum rule [3]. This type of disorder makes the formulation and numerical implementation

of an effective-medium theory for magnons rather demanding, as documented, e.g., by recent studies [4,5]. For these reasons, brute-force numerical approaches have often been used for magnon spectra and critical behavior of disordered ferromagnets, ranging from Monte Carlo simulations [5–7] over a direct solution of the spin dynamics equations [8] to a semianalytic real-space RPA [9–11].

These approaches have been quite successful in quantitative description of diluted magnetic semiconductors, such as Mn-doped GaAs [12]. As emphasized by several authors, this diluted system features a strong disorder which has a profound effect on its basic quantities, such as the Curie temperature T_C (see Refs. [6,7,10]) and the spin-wave stiffness D (see Ref. [11]). In particular, the high degree of dilution (content of Mn atoms below 10 at. %) makes the effects of local fluctuations very important. Depending on the Mn concentration and the spatial extent of the pair exchange interactions, percolation phenomena become important as well for Mn-doped GaAs and similar diluted ferromagnets. As a consequence, simple theoretical techniques, such as the MFA or the virtual-crystal approximation (VCA), fail to provide reliable values of T_C, D, and other physical quantities [12].

However, the very strong disorder cannot suppress all signs of phase coherence of the spin waves in Mn-doped GaAs. This feature has been observed and used in recent magneto-optical pump-and-probe experiments on (Ga,Mn)As epitaxial thin films [13,14], in which the stiffness D has been determined from frequencies of spin-wave resonances. This procedure rests on the original theory developed by Kittel for microscopically homogeneous ferromagnetic thin films with specific boundary conditions [15]. In the theoretical studies of Mn-doped GaAs, the spin-wave stiffness D has been derived from positions of peaks in the energy- and momentum-resolved magnon spectral function [5,11]; the employed periodic boundary conditions play only a technical role in these approaches. Let us note that a coherent component has also been found in the spectra of other excitations in

---

[*]turek@ipm.cz

[†]kudrnov@fzu.cz

[‡]drchal@fzu.cz

disordered media, such as, e.g., acoustic waves in granular systems [16,17].

The purpose of this paper is to examine theoretically spectral properties of spin waves of strongly disordered diluted ferromagnets in the long-wavelength limit from the point of view of the phase coherence. We find that this approach enables us to determine the spin-wave stiffness D without an intermediate calculation of the energy- and momentum-resolved spectral function. As an application, the values of D are studied for the (Ga,Mn)As, (Ga,Mn)(As,P), and (Ga,Mn)N diluted magnetic semiconductors in order to answer some actual questions, such as those related to the effect of doping by phosphorus on micromagnetic parameters of (Ga,Mn)As [14,18] and the relation between the spin stiffness and the Curie temperature [19].

II. MODELS AND METHODS

Our formalism employs the isotropic Heisenberg model for classical magnetic moments of the same fixed magnitude M located at lattice sites labeled by indices m,n,r. The energy of each configuration $\{\mathbf{e}_m\}$, where the unit vector $\mathbf{e}_m$ defines the direction of the local moment on site m, is given by

$$\mathcal{E} = -\sum_{mn} J_{mn}\mathbf{e}_m \cdot \mathbf{e}_n,\tag{1}$$

where the quantities J_{mn} denote the pair exchange interactions. They satisfy the usual properties ($J_{mm} = 0$, $J_{mn} = J_{nm}$) and are mostly nonnegative, so that the ground state is ferromagnetic. In the Green's function formalism [1,2,9,20,21], the zero-temperature spin-wave propagator is (apart from a prefactor) equivalent to the resolvent of the Hamiltonian H with matrix elements

$$H_{mn} = \delta_{mn}\left(\sum_r J_{mr}\right) - J_{mn},\tag{2}$$

and the energies of spin excitations are directly related to the eigenvalues of H. In the special case of a perfect crystalline ferromagnet on a Bravais lattice, the magnon energy for a reciprocal-space vector $\mathbf{q}$ can be obtained as

$$E^{\mathrm{mag}}(\mathbf{q}) = \frac{4\mu_{\mathrm{B}}}{M}[J(\mathbf{0}) - J(\mathbf{q})],\tag{3}$$

where μ_{B} is the Bohr magneton and the quantity $J(\mathbf{q})$ denotes the lattice Fourier transform of the translationally invariant pair exchange interactions J_{mn}. For lattices with a high-symmetry point group, such as the square lattice in two dimensions or fcc and bcc lattices in three dimensions, the magnon energy for small wave vectors $\mathbf{q}$ follows a quadratic law,

$$E^{\mathrm{mag}}(\mathbf{q}) \approx Dq^2,\tag{4}$$

where D is the spin-wave stiffness and $q = |\mathbf{q}|$.

The diluted ferromagnets considered in this study employ nonrandom translationally invariant pair exchange interactions J_{mn} defined on a Bravais lattice, but with the local moments occupying randomly only a part of all lattice sites. The concentration of the magnetic sites is denoted by x ($0 < x < 1$). We studied two different cases, both corresponding to long-range exchange interactions and a strong dilution ($x \ll 1$); the models were treated on large supercells with

periodic boundary conditions. The individual configurations were constructed by means of a random-number generator, and the eigenvalues of the Hamiltonian (2) were found numerically by means of standard techniques for the diagonalization of real symmetric matrices [22,23].

In the first case, a two-dimensional square lattice was chosen with the model exchange interaction

$$J_{mn} = A(a/d_{mn})^2 \exp(-d_{mn}/\lambda),\tag{5}$$

where A is the interaction strength, a denotes the lattice parameter, d_{mn} is the distance between lattice sites m and n, and λ denotes a screening length. The inverse proportionality to the square of the distance in the model (5) coincides with the nonoscillating part of the Ruderman-Kittel-Kasuya-Yosida interaction in two-dimensional metals [24], while the exponential decay with increasing distance reflects disorder-induced damping of the interaction. We choose $\lambda = 5a$ and neglect all interactions (5) for $d_{mn} > 35a$. Supercells of two shapes were constructed with an integer L controlling their size: (i) squares with edges La comprising L^2 sites ($100 \leqslant L \leqslant 300$) and (ii) rectangles with edges La and $2La$ comprising $2L^2$ sites ($75 \leqslant L \leqslant 180$). The concentration of local moments was chosen as $x = 0.03$; this small concentration is still above the percolation threshold owing to the big values of the screening length λ and the cutoff distance of the exchange interaction.

In the second case, realistic models of bulk Mn-doped GaAs were constructed with magnetic Mn atoms occupying randomly the fcc Ga sublattice of the zinc-blende structure of GaAs. The Mn-Mn exchange interactions were derived for each Mn concentration x ($x < 0.1$) from the *ab initio* electronic structure [25] using the magnetic force theorem [26]; the cutoff distance was taken as $6.36a$, where a denotes the lattice parameter of the zinc-blende structure. Supercells of two kinds were treated: (i) cubic supercells with edges La and with $4L^3$ fcc-lattice sites for Mn atoms ($18 \leqslant L \leqslant 38$) and (ii) rhombohedral supercells with edges given by three vectors, $(La/2,La/2,0)$, $(La/2,0,La/2)$, and $(0,La/2,La/2)$, which contain L^3 sites ($34 \leqslant L \leqslant 60$).

Reliable values of physical quantities follow from the supercell approach after averaging over N_{conf} random configurations; in agreement with previous studies [10,11], we found that $N_{\mathrm{conf}} = 50$ provides sufficient statistics in most cases. For the sake of comparison, results of the simple VCA will also be mentioned in the following. In the studied models, they are obtained by replacing the original pair interactions J_{mn} by concentration-weighted effective interactions xJ_{mn} (and by occupying the whole Bravais lattice by the local moments). As an example, we get from (3) the relation

$$E_{\mathrm{VCA}}^{\mathrm{mag}}(\mathbf{q}) = \frac{4\mu_{\mathrm{B}}}{M}x[J(\mathbf{0}) - J(\mathbf{q})],\tag{6}$$

representing the magnon energy in the VCA.

III. RESULTS AND DISCUSSION

A. Two-dimensional model

The distribution of eigenvalues E of the Hamiltonian (2) for the two-dimensional model can be inferred from Fig. 1, which displays the low-energy tail of the number-of-states function (integrated density of states) $N(E)$ averaged over
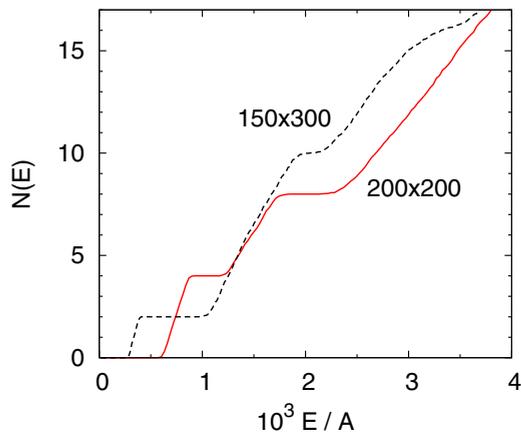
FIG. 1. The number of states $N(E)$ for the diluted 2D ferromagnet with 3% of magnetic sites simulated by a square supercell with 200×200 sites (solid line) and by a rectangular supercell with 150×300 sites (dashed line).

FIG. 2. The configurationally averaged lowest excitation energies E_1 for the diluted 2D ferromagnet as functions of the **q**-vector magnitude derived from the supercell size: for square supercells (open squares) and for rectangular supercells (solid diamonds). The straight dotted line results from a fit, and the dash-dotted line refers to the VCA dependence.

100 random configurations. The zero eigenvalue, present in each configuration due to general properties of the isotropic Heisenberg model (1), was omitted in the calculation of $N(E)$. The resulting $N(E)$ are featured by plateaus for supercells of both shapes (square and rectangular); these plateaus correspond to an absence of eigenvalues in certain energy intervals, which allows one to separate the first lowest excited levels (E_1) from higher-lying excitations. The constant values of $N(E)$ in the plateaus are integers, which point to four and two lowest excitations for the square and rectangular supercells, respectively.

Based on an analogy with spin waves in nonrandom ferromagnets treated with periodic boundary conditions [15], the lowest excitations E_1 can be ascribed to the shortest reciprocal-space vectors **q** compatible with the supercell shape and size. This identification yields four lowest excitations E_1 derived from the vectors given by $\mathbf{q} = 2\pi(\pm 1, 0)/(La)$ and $\mathbf{q} = 2\pi(0, \pm 1)/(La)$ for the square supercells, but only two lowest excitations are obtained from $\mathbf{q} = \pi(0, \pm 1)/(La)$ for the rectangular supercells employed. These integers coincide with the constant $N(E)$ values inside the plateaus (see Fig. 1).

This interpretation of the plateaus in $N(E)$ is further corroborated by the dependence of the configurationally averaged value of E_1 on the shortest **q**-vector magnitude, as obtained from variations of the supercell size L and plotted in Fig. 2. One can see a proportionality relation $E_1 = k_1 q^2$ for both shapes, with a common slope k_1 equivalent to the spin-wave stiffness D (note that $D/k_1 = 4\mu_B/M$). The stiffness from the supercell calculations is significantly reduced compared to its VCA counterpart (Fig. 2), in qualitative agreement with recent results for a diluted two-dimensional ferromagnet [27] with a slightly different distance dependence of the pair exchange interaction ($J_{mn} \propto d_{mn}^{-3}$). A similar overestimation of D in the VCA has also been observed for the exchange interaction restricted to the first nearest neighbors but with a much higher concentration of magnetic atoms [5]. These facts can be understood in terms of the lowest moments of the **q**-dependent magnon spectral function: its mean value, given by the first moment and identical to the excitation energy in the
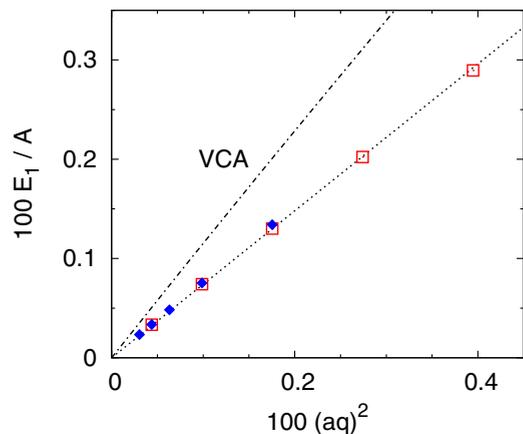
VCA, is comparable to the linewidth (the standard deviation of the spectral function), given by the second moment (see Ref. [11] for details).

The results shown in Figs. 1 and 2 prove that the dispersion law of low-energy spin excitations can easily be obtained only from the sensitivity of the lowest eigenvalues of the Hamiltonian (2) to the adopted boundary conditions of the simulation supercells. This sensitivity reflects the coherent part of the magnon spectrum, which is present despite the strong disorder and dilution. Theoretically, the presence of the coherent part rests on a very weak damping of low-energy magnons (see Ref. [27] and references therein). The developed numerical approach can be used for diluted and concentrated random ferromagnets, and it does not require a computation of the eigenvectors of the matrix (2); its particular numerical efficiency for diluted systems is due to a much smaller number of magnetic atoms compared to the total number of lattice sites in the supercell.

B. Bulk (Ga,Mn)As and (Ga,Mn)(As,P)

The low-energy tail of the number-of-states function $N(E)$ for GaAs doped by 5% Mn atoms is shown in Fig. 3. Like in the previous case (Fig. 1), plateaus in $N(E)$ are present for both kinds of supercells. The constant values of $N(E)$ in the first plateaus amount to six and eight for the cubic and rhombohedral supercells, respectively. These integer values can again be explained in terms of the shortest reciprocal-space vectors derived from the supercell shape and size: there are six vectors equivalent to the vector $\mathbf{q} = 2\pi(1, 0, 0)/(La)$ for the cubic supercell, while eight vectors equivalent to the vector $\mathbf{q} = 2\pi(1, 1, 1)/(La)$ correspond to the rhombohedral supercell. Note that in the case of the rhombohedral supercell, the plateau separating the first and the second lowest eigenvalues is quite narrow since the magnitude of the second shortest **q** vector, given by $\mathbf{q} = 4\pi(1, 0, 0)/(La)$, exceeds only slightly that of the first shortest vector. However, a separation between
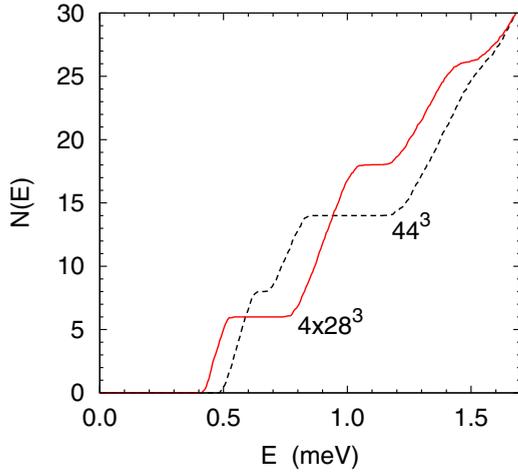
FIG. 3. The number of states $N(E)$ for GaAs doped by 5% Mn simulated by a cubic supercell with 4×28^3 sites (solid line) and by a rhombohedral supercell with 44^3 sites (dashed line).

the second and third shortest vectors is clearly visible for both kinds of supercells (Fig. 3).

The dependence of the average value E_1 of the six (cubic supercell) or eight (rhombohedral supercell) lowest excitation energies on the size of the shortest **q** vector, obtained with variations of L for the same system, is displayed in Fig. 4. The relation $E_1 \propto q^2$ with a slope independent of the supercell shape is clearly visible again, in analogy with the two-dimensional model (Fig. 2); this slope is markedly smaller than the value derived from the VCA magnon dispersion law (6). The overestimation of the VCA with respect to the numerically obtained slope (spin stiffness) for Mn-doped GaAs was revealed originally by Bouzerar [11].

The calculated spin-wave stiffness D of bulk $(Ga_{1-x}Mn_x)As$ as a function of Mn concentration x is displayed in Fig. 5 together with recent experimental values
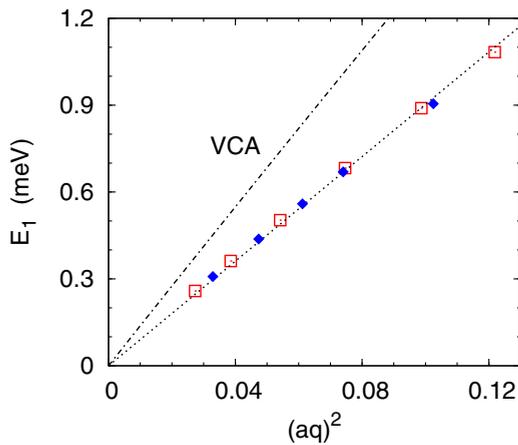
FIG. 4. The configurationally averaged lowest excitation energies E_1 for Mn-doped GaAs as functions of the **q**-vector magnitude derived from the supercell size for cubic supercells (open squares) and for rhombohedral supercells (solid diamonds). The straight dotted line results from a fit, and the dash-dotted line refers to the VCA dependence.
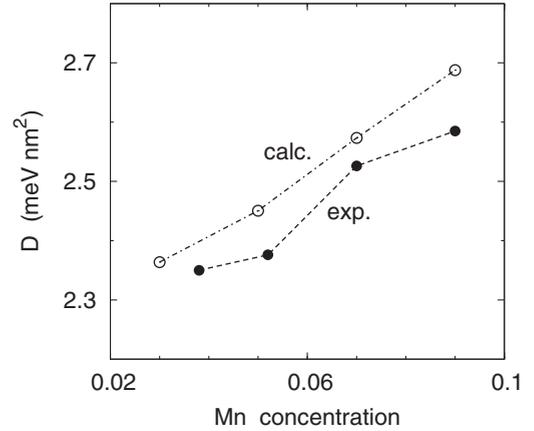
FIG. 5. The calculated spin-wave stiffness D as a function of Mn concentration in (Ga,Mn)As (open circles). The experimental values (solid circles) [13] are shown as well.

obtained for epitaxial thin films with a small number of compensating defects [13]. It should be noted that typical sizes q of wave vectors relevant in the magneto-optical pump-and-probe experiment, which are given by the thickness of prepared epitaxial films and by an integer index of the observed resonance mode, are characterized by $aq \gtrsim 0.04$ [13], which includes values smaller than those used in the numerical simulations, $aq \gtrsim 0.17$ (Fig. 4). In spite of this difference, one can see satisfactory agreement between the theory and experiment both in the magnitude and in the slope of the concentration dependence of D (Fig. 5). The present values of D are quite close to the results obtained by Bouzerar [11], which were based on the same *ab initio* exchange interactions (with a smaller cutoff distance than in this study) and on the peaks of the magnon spectral function, whereas a more recent model study, including effects of spin-orbit coupling on the exchange interactions, led to appreciably smaller spin stiffnesses [19].

Among other diluted ferromagnets related to (Ga,Mn)As, the quaternary (Ga,Mn)(As,P) alloy, where P atoms substitute As atoms on the anion sublattice of the zinc-blende structure, has recently been investigated both theoretically [28,29] and experimentally [14,18]; its chemical composition can be summarized as $(Ga_{1-x}Mn_x)(As_{1-y}P_y)$. The experimental study of alloys with 6% Mn has indicated that incorporation of 10% phosphorus leads to a pronounced reduction of the spin-wave stiffness: values of $D = (2.5 \pm 0.2)$ meV nm^2 and $D = (1.9 \pm 0.2)$ meV nm^2 for $y = 0$ and $y = 0.1$, respectively, were reported [18]. However, this effect of P doping has not been confirmed in another study of samples of similar compositions [14].

We have studied the spin-wave stiffness D for $y = 0$ and $y = 0.1$ with a fixed Mn concentration, $x = 0.06$. The P-doped system was treated with two different lattice parameters, first, with the same a as that of the P-free system (identical to that of pure GaAs, $a = 0.565$ nm) and, second, with a slightly smaller value ($a = 0.563$ nm) which reflects the smaller lattice of pure GaP ($a = 0.545$ nm) compared to GaAs. The reference value of D for the P-free system ($y = 0$) was $D = 2.52$ meV nm^2, while for the P-doped system ($y = 0.1$),

values of $D = 2.48$ meV nm^2 and $D = 2.47$ meV nm^2 were obtained. The corresponding values of the Curie temperature, calculated in the real-space RPA [9], are $T_C = (124 \pm 1)$ K for $y = 0$ and $T_C = (122 \pm 1)$ K for $y = 0.1$ (irrespective of a). The calculated results thus agree with the observed negligible sensitivity of D to alloying by phosphorus [14]; the origin of the reduction of D, reported in Ref. [18], might be ascribed to additional compensating defects induced by P doping which should also reduce the T_C. This explanation is in line with the measured Curie temperatures [18]: $T_C \approx 130$ K for $y = 0$ and $T_C \approx 110$ K for $y = 0.1$, which is in contrast to the very small change in the calculated T_C due to the incorporation of phosphorus, as found also in a previous theoretical study [28].

C. Relation between spin-wave stiffness and Curie temperature

The spin-wave stiffness D is related naturally to the low-temperature properties of a ferromagnet, in contrast to the Curie temperature T_C as a basic finite-temperature quantity. The mutual relation of D and T_C has been experimentally investigated, e.g., for Co-based Heusler alloys [30]. On the theoretical side, a proportionality between both quantities can be derived; this derivation rests on a mean-field treatment for T_C and on the nearest-neighbor nature of the exchange interaction (see Ref. [19] and references therein). Since the MFA is not accurate enough for diluted systems, where the spatial range of J_{mn} plays an important role, the relation between D and T_C has been addressed in several studies, including diluted metallic Pd-based alloys [31] and the (Ga,Mn)As system [11,19]. In order to get a deeper insight into this topic, we have also applied the developed theory to Mn-doped GaN alloys treated in the cubic zinc-blende structure [6,7,32]. Since the exchange interactions in (Ga,Mn)N are much more localized than in (Ga,Mn)As, a smaller cutoff distance of $4a$ could be used for reliable numerical values. The Mn concentration x in $(Ga_{1-x}Mn_x)N$ was limited to $0.02 \leqslant x \leqslant 0.06$ in order to avoid a negative exchange interaction between the second nearest Mn-Mn neighbors which appears for higher Mn contents [7,32].
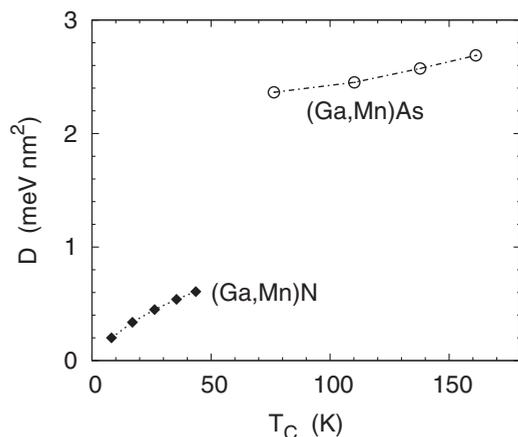
FIG. 6. Correlations between the Curie temperature T_C and the spin-wave stiffness D as calculated for (Ga,Mn)As (open circles) and (Ga,Mn)N (solid diamonds).
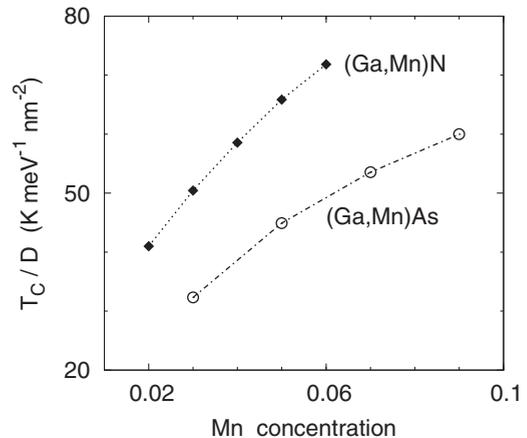
FIG. 7. The ratio T_C/D as a function of Mn concentration for (Ga,Mn)As (open circles) and (Ga,Mn)N (solid diamonds).

The values of the Curie temperature were obtained with the real-space RPA [9] for both systems. The calculated T_C for (Ga,Mn)As compare reasonably well with the experiment for carefully prepared samples [13] (see a recent study for more details [33]). The obtained T_C for (Ga,Mn)N are very close to the results of Ref. [32], which employed the same RPA approach; Monte Carlo simulations yield Curie temperatures in the studied concentration interval both slightly above [6] and slightly below [7] the present values.

The resulting correlations between D and T_C are displayed in Fig. 6 for both systems. One can see not only appreciably different values for the two ferromagnets but also qualitatively different trends. However, the ratio T_C/D, plotted in Fig. 7, exhibits quite similar values and qualitatively identical concentration dependences in both cases studied. Let us note that the same concentration trend of T_C/D, namely, its decrease with decreasing x and its concave shape, was reported previously for (Ga,Mn)As [11]. The present analysis allows one to extend this conclusion also to (Ga,Mn)N, despite the markedly stronger spatial localization of the underlying exchange interactions.

IV. CONCLUSIONS

We have proved that diluted ferromagnets with long-range exchange interactions possess spin-wave spectra with a nonvanishing coherent part in the low-energy region. This coherence leads to interference effects which are not suppressed by the strong disorder of the diluted system. We have shown that these features can be employed in numerical simulations to determine the spin-wave stiffness without any recourse to the magnon spectral function. Our approach represents a simple and efficient way in the case of diluted systems that is complementary to a recent sophisticated theory applicable also to concentrated random ferromagnets [5].

In combination with existing first-principles techniques for calculations of the exchange interactions, we studied selected diluted magnetic III–V semiconductors. Besides the theoretical reproduction of the measured spin stiffness in optimally synthesized (Ga,Mn)As samples and of its negligible sensitivity to the doping by phosphorus, we found that the

ratio of the Curie temperature to the spin stiffness follows qualitatively the same concentration trend independent of the degree of localization of the Mn-Mn exchange interactions.

This pilot study was limited to highly symmetric (square and cubic) structures and to ideal models of diluted ferromagnets within the isotropic Heisenberg Hamiltonian. Consequently, straightforward extensions can be considered in the following directions: (i) the presence of compensating defects, atomic short-range order, or chemical inhomogeneities, (ii) cases with less symmetric structures, such as the hexagonal wurtzite structure relevant for (Ga,Mn)N, and (iii) spin models with anisotropic exchange interactions owing to relativistic effects. However, possible generalization of the developed approach is less obvious for solving more difficult problems, such as a treatment of ferromagnetic and antiferromagnetic exchange interactions, which modify the ground state of a random magnet (a spin-glass state) and its excitation spectrum, or investigation of the disorder-induced damping of the spin waves (finite lifetimes of magnons), addressed recently by means of the spectral function [27]. Clarification of these points has to be left for future studies.

[1] S. V. Tyablikov, *Methods in the Quantum Theory of Magnetism* (Plenum, New York, 1967).

[2] N. Majlis, *The Quantum Theory of Magnetism* (World Scientific, Singapore, 2000).

[3] A. Gonis, *Theoretical Materials Science* (Materials Research Society, Warrendale, PA, 2000).

[4] G. Bouzerar and P. Bruno, Phys. Rev. B **66**, 014410 (2002).

[5] P. Buczek, L. M. Sandratskii, N. Buczek, S. Thomas, G. Vignale, and A. Ernst, Phys. Rev. B **94**, 054407 (2016).

[6] L. Bergqvist, O. Eriksson, J. Kudrnovský, V. Drchal, P. Korzhavyi, and I. Turek, Phys. Rev. Lett. **93**, 137202 (2004).

[7] K. Sato, W. Schweika, P. H. Dederichs, and H. Katayama-Yoshida, Phys. Rev. B **70**, 201202(R) (2004).

[8] B. Skubic, J. Hellsvik, L. Nordström, and O. Eriksson, J. Phys. Condens. Matter **20**, 315203 (2008).

[9] S. Hilbert and W. Nolting, Phys. Rev. B **70**, 165203 (2004).

[10] G. Bouzerar, T. Ziman, and J. Kudrnovský, Europhys. Lett. **69**, 812 (2005).

[11] G. Bouzerar, Europhys. Lett. **79**, 57007 (2007).

[12] K. Sato, L. Bergqvist, J. Kudrnovský, P. H. Dederichs, O. Eriksson, I. Turek, B. Sanyal, G. Bouzerar, H. Katayama-Yoshida, V. A. Dinh, T. Fukushima, H. Kizaki, and R. Zeller, Rev. Mod. Phys. **82**, 1633 (2010).

[13] P. Němec, V. Novák, N. Tesařová, E. Rozkotová, H. Reichlová, D. Butkovičová, F. Trojánek, K. Olejník, P. Malý, R. P. Campion, B. L. Gallagher, J. Sinova, and T. Jungwirth, Nat. Commun. **4**, 1422 (2013).

[14] S. Shihab, H. Riahi, L. Thevenard, H. J. von Bardeleben, A. Lemaître, and C. Gourdon, Appl. Phys. Lett. **106**, 142408 (2015).

[15] C. Kittel, Phys. Rev. **110**, 1295 (1958).

[16] X. Jia, C. Caroli, and B. Velický, Phys. Rev. Lett. **82**, 1863 (1999).

[17] E. Somfai, J.-N. Roux, J. H. Snoeijer, M. van Hecke, and W. van Saarloos, Phys. Rev. E **72**, 021301 (2005).

[18] N. Tesařová, D. Butkovičová, R. P. Campion, A. W. Rushforth, K. W. Edmonds, P. Wadley, B. L. Gallagher, E. Schmoranzerová, F. Trojánek, P. Malý, P. Motloch, V. Novák, T. Jungwirth, and P. Němec, Phys. Rev. B **90**, 155203 (2014).

[19] A. Werpachowska and T. Dietl, Phys. Rev. B **82**, 085204 (2010).

[20] J. Rusz, I. Turek, and M. Diviš, Phys. Rev. B **71**, 174408 (2005).

[21] E. Şaşıoğlu, L. M. Sandratskii, P. Bruno, and I. Galanakis, Phys. Rev. B **72**, 184415 (2005).

[22] J. H. Wilkinson, *The Algebraic Eigenvalue Problem* (Clarendon, Oxford, 1965).

[23] W. H. Press, S. A. Teukolsky, W. T. Vetterling, and B. P. Flannery, *Numerical Recipes in FORTRAN* (Cambridge University Press, Cambridge, 1992).

[24] B. Fischer and M. W. Klein, Phys. Rev. B **11**, 2025 (1975).

[25] J. Kudrnovský, I. Turek, V. Drchal, F. Máca, P. Weinberger, and P. Bruno, Phys. Rev. B **69**, 115208 (2004).

[26] A. I. Liechtenstein, M. I. Katsnelson, V. P. Antropov, and V. A. Gubanov, J. Magn. Magn. Mater. **67**, 65 (1987).

[27] A. Chakraborty, P. Wenk, and J. Schliemann, Eur. Phys. J. B **88**, 64 (2015).

[28] J. L. Xu and M. van Schilfgaarde, J. Magn. Magn. Mater. **305**, 63 (2006).

[29] J. Mašek, J. Kudrnovský, F. Máca, J. Sinova, A. H. MacDonald, R. P. Campion, B. L. Gallagher, and T. Jungwirth, Phys. Rev. B **75**, 045202 (2007).

[30] R. Y. Umetsu, A. Okubo, A. Fujita, T. Kanomata, K. Ishida, and R. Kainuma, IEEE Trans. Magn. **47**, 2451 (2011).

[31] I. Y. Korenblit and E. F. Shender, Sov. Phys. JETP **44**, 819 (1976).

[32] S. Hilbert and W. Nolting, Phys. Rev. B **71**, 113204 (2005).

[33] J. Kudrnovský, V. Drchal, and I. Turek, Phys. Rev. B **94**, 054428 (2016).